Journal of Computational and Applied Mathematics 236 (2012) 4462–4473

Contents lists available at SciVerse ScienceDirect

Journal of Computational and Applied Mathematics

journal homepage: www.elsevier.com/locate/cam

High-order compact finite difference scheme for option pricing in stochastic volatility models

Bertram Düring [a,*], Michel Fournié [b]

[a] Department of Mathematics, University of Sussex, Pevensey II, Brighton, BN1 9QH, United Kingdom

[b] Institut de Mathématiques de Toulouse, Université de Toulouse et CNRS (UMR 5219), France

ARTICLE INFO

Article history:
Received 23 July 2010
Received in revised form 16 April 2012

MSC:
65M06
65M12
91B28

Keywords:
Option pricing
Compact finite difference discretisations
Mixed derivatives
High-order scheme

ABSTRACT

We derive a new high-order compact finite difference scheme for option pricing in stochastic volatility models. The scheme is fourth order accurate in space and second order accurate in time. Under some restrictions, theoretical results like unconditional stability in the sense of von Neumann are presented. Where the analysis becomes too involved we validate our findings by a numerical study. Numerical experiments for the European option pricing problem are presented. We observe fourth order convergence for non-smooth payoff.

1. Introduction

The traditional approach to price derivative assets or options is to specify an asset price process exogenously by a stochastic diffusion process and then price by no-arbitrage arguments. The seminal example of this approach is Black and Scholes' paper [1] on pricing of European-style options. This approach leads to simple, explicit pricing formulas. However, empirical research has revealed that they are not able to explain important effects in real financial markets, e.g. the volatility smile (or skew) in option prices.

In real financial markets, not only asset returns are subject to risk, but also the estimate of the riskiness is typically subject to significant uncertainty. To incorporate such an additional source of randomness into an asset pricing model, one has to introduce a second risk factor. This also allows to fit higher moments of the asset return distribution. The most prominent work in this direction is the Heston model [2]. Such models are based on a two-dimensional stochastic diffusion process with two Brownian motions with correlation ρ, i.e. $dW^{(1)}(t)dW^{(2)}(t) = \rho\, dt$, on a given filtered probability space for the stock price $S = S(t)$ and the stochastic volatility $\sigma = \sigma(t)$

$$dS(t) = \bar{\mu} S(t)\, dt + \sqrt{\sigma(t)} S(t)\, dW^{(1)}(t),$$
$$d\sigma(t) = a(\sigma(t))\, dt + b(\sigma(t))\, dW^{(2)}(t),$$

where $\bar{\mu}$ is the drift of the stock, $a(\sigma)$ and $b(\sigma)$ are the drift and the diffusion coefficient of the stochastic volatility.

* Corresponding author.
E-mail addresses: b.during@sussex.ac.uk (B. Düring), michel.fournie@math.univ-toulouse.fr (M. Fournié).

0377-0427/$ – see front matter © 2012 Elsevier B.V. All rights reserved.
doi:10.1016/j.cam.2012.04.017

Application of Itô's lemma leads to partial differential equations of the following form

$$V_t + \frac{1}{2}S^2\sigma V_{SS} + \rho b(\sigma)\sqrt{\sigma}SV_{S\sigma} + \frac{1}{2}b^2(\sigma)V_{\sigma\sigma} + a(\sigma)V_\sigma + rSV_S - rV = 0, \tag{1}$$

where r is the (constant) riskless interest rate. Eq. (1) has to be solved for $S, \sigma > 0,\ 0 \le t \le T$ and subject to final and boundary conditions which depend on the specific option that is to be priced.

For some models and under additional restrictions, closed form solutions to (1) can be obtained by Fourier methods (e.g. [2,3]). Another approach is to derive approximate analytic expressions, see e.g. [4] and the literature cited therein. In general, however – even in the Heston model [2] when the parameters in it are non constant – Eq. (1) has to be solved numerically. Moreover, many (so-called American) options feature an additional early exercise right. Then one has to solve a free boundary problem which consists of (1) and an early exercise constraint for the option price. Also for this problem one typically has to resort to numerical approximations.

In the mathematical literature, there are many papers on numerical methods for option pricing, mostly addressing the one-dimensional case of a single risk factor and using standard, second order finite difference methods (see, e.g. [5] and the references therein). More recently, high-order finite difference schemes (fourth order in space) were proposed that use a compact stencil (three points in space). In the present context see, e.g. [6] for linear and [7–9] for fully nonlinear problems.

There are less works considering numerical methods for option pricing in stochastic volatility models, i.e. for two spatial dimensions. Finite difference approaches that are used are often standard, low order methods (second order in space) and do provide little numerical analysis or convergence results. Other approaches include finite element–finite volume [10], multigrid [11], sparse wavelet [12], or spectral methods [13].

Let us review some of the related finite difference literature. Different efficient methods for solving the American option pricing problem for the Heston model are compared in [14]. The article focuses on the treatment of the early exercise free boundary and uses a second order finite difference discretisation. In [15] different, low order ADI (alternating direction implicit) schemes are adapted to the Heston model to include the mixed spatial derivative term. While most of [6] focuses on high-order compact scheme for the standard (one-dimensional) case, in a short remark [6, Section 5] the stochastic volatility (two-dimensional) case is also considered. However, the final scheme there is of second order only due to the low order approximation of the cross diffusion term.

The originality of the present work consists in proposing a new, *high-order compact finite difference scheme* for (two-dimensional) option pricing models with *stochastic volatility*. It should be emphasised that although our presentation is focused on the Heston model, our methodology naturally adapts to other stochastic volatility models. We derive a new compact scheme that is fourth order accurate in space and second order accurate in time. The stability analysis of the scheme is a difficult task due to the multi-dimensional context, variable coefficients and the nature of the boundary conditions. Under additional assumptions (zero correlation, periodic boundary conditions), we establish theoretical results like unconditional stability in the sense of von Neumann (for 'frozen coefficients'). We discuss this in the numerical part.

This paper is organised as follows. In the next section, we recall the Heston model from [2] and its closed form solution for the constant parameters case. In Section 3 we introduce new independent variables to transform the partial differential equation to a more tractable form. In Section 4 we derive the new high-order compact scheme. We analyse its necessary stability condition in Section 4.3. Numerical experiments that confirm the good properties of the method are presented in Section 5. We give numerical results for the European option pricing problem with non-smooth payoff and observe fourth order convergence. Section 6 concludes.

2. Heston model

Let us recall the Heston model from [2] on which we will focus our presentation. Consider a two-dimensional standard Brownian motion $W = (W^{(1)}, W^{(2)})$ with correlation $dW^{(1)}(t)dW^{(2)}(t) = \rho dt$ on a given filtered probability space. Assuming a specific form of the drift $a(\sigma)$ and the diffusion coefficient $b(\sigma)$ of the stochastic volatility, the value of the underlying asset in [2] is characterised by

$$\begin{aligned} dS(t) &= \bar{\mu}S(t)\,dt + \sqrt{\sigma(t)}S(t)\,dW^{(1)}(t), \\ d\sigma(t) &= \kappa^*(\theta^* - \sigma(t))\,dt + v\sqrt{\sigma(t)}\,dW^{(2)}(t), \end{aligned} \tag{2}$$

for $0 < t \le T$ with $S(0), \sigma(0) > 0$ and $\bar{\mu}$, κ^*, v and θ^* the drift, the mean reversion speed, the volatility of volatility and the long-run mean of σ, respectively.

Note that our method carries over to other stochastic volatility models with different choices of the drift and the diffusion coefficient of the stochastic volatility, e.g. the GARCH diffusion model

$$d\sigma(t) = \kappa^*(\theta^* - \sigma(t))\,dt + v\sigma(t)\,dW^{(2)}(t), \tag{3}$$

or the so-called 3/2-model

$$d\sigma(t) = \kappa^*\sigma(t)(\theta^* - \sigma(t))\,dt + v\sigma(t)^{3/2}\,dW^{(2)}(t), \tag{4}$$

in a natural way (see also Remark 1 at the end of Section 4.1).

In the Heston model, it follows by Itô's lemma and standard arbitrage arguments that any derivative asset $V = V(S, \sigma, t)$ solves the following partial differential equation

$$V_t + \frac{1}{2}S^2\sigma V_{SS} + \rho v\sigma S V_{S\sigma} + \frac{1}{2}v^2\sigma V_{\sigma\sigma} + rSV_S + \big[\kappa^*(\theta^* - \sigma) - \lambda(S, \sigma, t)\big]V_\sigma - rV = 0, \tag{5}$$

which has to be solved for $S, \sigma > 0,\ 0 \le t < T$ and subject to a suitable final condition, e.g.

$$V(S, \sigma, T) = \max(K - S, 0),$$

in case of a European put option (with K denoting the strike price). In (5), $\lambda(S, \sigma, t)$ denotes the market price of volatility risk. While in principle it could be estimated from market data, this is difficult in practice and the results are controversial. Therefore, one typically assumes a risk premium that is proportional to σ and chooses $\lambda(S, \sigma, t) = \lambda_0\sigma$ for some constant λ_0. For streamlining the presentation we restrict ourselves to this important case, although our scheme applies to general functional forms $\lambda = \lambda(S, \sigma, t)$.

The 'boundary' conditions in the case of the put option read as follows

$$V(0, \sigma, t) = Ke^{-r(T-t)}, \quad T > t \ge 0,\ \sigma > 0, \tag{6a}$$
$$V(S, \sigma, t) \to 0, \quad T > t \ge 0,\ \sigma > 0,\ \text{as } S \to \infty, \tag{6b}$$
$$V_\sigma(S, \sigma, t) \to 0, \quad T > t \ge 0,\ S > 0,\ \text{as } \sigma \to \infty. \tag{6c}$$

The remaining boundary condition at $\sigma = 0$ can be obtained by looking at the formal limit $\sigma \to 0$ in (5),

$$V_t + rSV_S + \kappa^*\theta^*V_\sigma - rV = 0, \quad T > t \ge 0,\ S > 0,\ \text{as } \sigma \to 0. \tag{6d}$$

This boundary condition is used frequently, e.g. in [14,10]. Alternatively, one can use a homogeneous Neumann condition [11],

$$V_\sigma(S, \sigma, t) \to 0, \quad T > t \ge 0,\ S > 0,\ \text{as } \sigma \to 0. \tag{6e}$$

For *constant* parameters, one can employ Fourier transform techniques and obtain a system of ordinary differential equations which can be solved analytically [2]. By inverting the transform one arrives at a closed-form solution of (5), where the European put option price V is given by

$$V(S, \sigma, t) = Ke^{-r(T-t)}P_2 - SP_1, \tag{7}$$

with $(k = 1, 2)$

$$P_k = \frac{1}{2} + \frac{1}{\pi}\int_0^\infty \mathrm{Re}\left[\frac{e^{-i\xi\ln(K)}f_k(\xi)}{i\xi}\right]d\xi, \tag{8}$$
$$f_k(\xi) = \exp\big(C_k(T-t, \xi) + \sigma D_k(T-t, \xi) + i\xi\ln S\big),$$
$$C_k(\tau, \xi) = r\xi i\tau + \frac{\kappa^*\theta^*}{v^2}\left[(b_k + d_k)\tau - 2\ln\Big(\frac{1 - ge^{d_k\tau}}{1 - g}\Big)\right], \qquad D_k(\tau, \xi) = \frac{b_k + d_k}{v^2}\frac{1 - e^{d_k\tau}}{1 - ge^{d_k\tau}},$$
$$g = \frac{b_k + d_k}{b_k - d_k}, \quad d_k = \sqrt{\big(\xi^2 \mp i\xi\big)\,v^2 + b_k^2},\ b_k = \kappa^* + \lambda_0 - \rho v(i\xi + \delta_{1k}).$$

Here, $\delta_{i,j}$ denotes Kronecker's delta.

3. Transformation of the equation and boundary conditions

Under the transformation of variables

$$x = \ln\Big(\frac{S}{K}\Big), \qquad \tilde{t} = T - t, \qquad u = \exp(r\tilde{t})\frac{V}{K}, \tag{9}$$

(we immediately drop the tilde in the following) we arrive at

$$u_t - \frac{1}{2}\sigma\big(u_{xx} + 2\rho v u_{x\sigma} + v^2 u_{\sigma\sigma}\big) + \Big(\frac{1}{2}\sigma - r\Big)u_x - \big[\kappa^*\theta^* - (\kappa^* + \lambda_0)\sigma\big]u_\sigma = 0, \tag{10}$$

which is now posed on $\mathbb{R} \times \mathbb{R}^+ \times (0, T)$. We study the problem using the modified parameters

$$\kappa = \kappa^* + \lambda_0, \qquad \theta = \frac{\kappa^*\theta^*}{\kappa^* + \lambda_0},$$

which is both convenient and standard practice. For similar reasons, some authors set the market price of volatility risk to zero. Eq. (10) can then be written as

$$u_t - \frac{1}{2}\sigma\left(u_{xx} + 2\rho v u_{x\sigma} + v^2 u_{\sigma\sigma}\right) + \left(\frac{1}{2}\sigma - r\right)u_x - \kappa\left[\theta - \sigma\right]u_\sigma = 0. \tag{11}$$

The problem is completed by the following initial and boundary conditions:

$$\begin{aligned}
&u(x,\sigma,0) = \max(1-\exp(x),0), \quad x\in\mathbb{R},\ \sigma>0,\\
&u(x,\sigma,t)\to 1, \quad x\to-\infty,\ \sigma>0,\ t>0,\\
&u(x,\sigma,t)\to 0, \quad x\to+\infty,\ \sigma>0,\ t>0,\\
&u_\sigma(x,\sigma,t)\to 0, \quad x\in\mathbb{R},\ \sigma\to\infty,\ t>0,\\
&u_\sigma(x,\sigma,t)\to 0, \quad x\in\mathbb{R},\ \sigma\to 0,\ t>0.
\end{aligned}$$

4. High-order compact scheme

For the discretisation, we replace $\mathbb{R}$ by $[-R_1, R_1]$ and $\mathbb{R}^+$ by $[L_2, R_2]$ with $R_1, R_2 > L_2 > 0$. For simplicity, we consider a uniform grid $Z = \{x_i \in [-R_1, R_1] :\ x_i = ih_1, i = -N,\dots,N\} \times \{\sigma_j \in [L_2, R_2] :\ \sigma_j = L_2 + jh_2,\ j = 0,\dots,M\}$ consisting of $(2N+1)\times(M+1)$ grid points, with $R_1 = Nh_1,\ R_2 = L_2 + Mh_2$ and with space steps h_1, h_2 and time step k. Let $u^n_{i,j}$ denote the approximate solution of (11) in (x_i, σ_j) at the time $t_n = nk$ and let $u^n = (u^n_{i,j})$.

We impose artificial boundary conditions in a classical manner rigorously studied for a class of Black–Scholes equations in [16]. The boundary conditions on the grid are treated as follows. Due to the compactness of the scheme, the treatment of the Dirichlet boundary conditions is minimal. It is straightforward to consider Dirichlet boundary conditions without introduction of numerical error by imposing

$$u^n_{-N,j} = 1 - e^{rt_n - Nh}, \qquad u^n_{+N,j} = 0, \quad (j = 0,\dots,M).$$

At the other boundaries we impose homogeneous Neumann boundary conditions. The treatment of homogeneous Neumann conditions requires more attention. Indeed, no values are prescribed. The values of the unknown on the boundaries must be set by extrapolation from values in the interior. Then a numerical error is introduced, and the main consideration is that the order of extrapolation should be high enough not to affect the overall order of accuracy. We refer to the paper of Gustafsson [17] to discuss the influence of the order of the approximation on the global convergence rate and justify our choice of fourth order extrapolation formulae. By the Taylor expansion, if we cancel the first derivates on the boundaries, it is trivial to verify

$$u^n_{i,0} = \frac{18}{11}u^n_{i,1} - \frac{9}{11}u^n_{i,2} + \frac{2}{11}u^n_{i,3}, \quad (i = -N+1,\dots,N-1),$$

and

$$u^n_{i,M} = \frac{18}{11}u^n_{i,M-1} - \frac{9}{11}u^n_{i,M-2} + \frac{2}{11}u^n_{i,M-3}, \quad (i = -N+1,\dots,N-1).$$

4.1. Derivation of the high-order scheme for the elliptic problem

First we introduce the high-order compact finite difference discretisation for the stationary, elliptic problem with Laplacian operator which appears after the variable transformation $y = \sigma/v$. Eq. (11) is then reduced to the two-dimensional elliptic equation

$$-\frac{1}{2}vy(u_{xx} + u_{yy}) - \rho v y u_{xy} + \left(\frac{1}{2}vy - r\right)u_x - \kappa\frac{\theta - vy}{v}u_y = f(x,y), \tag{12}$$

with the same boundary conditions.

The fourth order compact finite difference scheme uses a nine-point computational stencil using the eight nearest neighbouring points of the reference grid point (i, j).

The idea behind the derivation of the high-order compact scheme is to operate on the differential equations as an auxiliary relation to obtain finite difference approximations for high-order derivatives in the truncation error. Inclusion of these expressions in a central difference method for Eq. (12) increases the order of accuracy, typically to $\mathcal{O}(h^4)$, while retaining a compact stencil defined by nodes surrounding a grid point.

Introducing a uniform grid with mesh spacing $h = h_1 = h_2$ in both the x- and y-direction, the standard central difference approximation to Eq. (12) at grid point (i, j) is

$$-\frac{1}{2}vy_j\left(\delta_x^2 u_{i,j} + \delta_y^2 u_{i,j}\right) - \rho v y_j \delta_x\delta_y u_{i,j} + \left(\frac{1}{2}vy_j - r\right)\delta_x u_{i,j} - \kappa\frac{\theta - vy_j}{v}\delta_y u_{i,j} - \tau_{i,j} = f_{i,j}, \tag{13}$$

where δ_x and δ_x^2 (δ_y and δ_y^2, respectively) denote the first and second order central difference approximations with respect to x (with respect to y). The associated truncation error is given by

$$\tau_{i,j} = \frac{1}{24} v y h^2 (u_{xxxx} + u_{yyyy}) + \frac{1}{6} \rho v y h^2 (u_{xyyy} + u_{xxxy}) + \frac{1}{12} (2r - vy) h^2 u_{xxx} + \frac{1}{6} \frac{\kappa(\theta - vy)}{v} h^2 u_{yyy} + \mathcal{O}(h^4). \tag{14}$$

For the sake of readability, here and in the following we omit the subindices j and (i, j) on y_j and $u_{i,j}$ (and its derivatives), respectively. We now seek second-order approximations to the derivatives appearing in (14). Differentiating Eq. (12) once with respect to x and y, respectively, yields

$$u_{xxx} = -u_{xyy} - 2\rho u_{xxy} - \frac{2r + vy}{vy} u_{xx} + 2\frac{\kappa(vy - \theta)}{v^2 y} u_{xy} - \frac{2}{vy} f_x, \tag{15}$$

$$u_{yyy} = -u_{xxy} - 2\rho u_{xyy} - \frac{1}{y} u_{xx} - \frac{2\kappa(\theta - vy) + v^2}{v^2 y} u_{yy} - \frac{2\rho + 2r - vy}{vy} u_{xy} + \frac{1}{y} u_x + \frac{2\kappa}{vy} u_y - \frac{2}{vy} f_y. \tag{16}$$

Differentiating Eqs. (15) and (16) with respect to y and x, respectively, and adding the two expressions, we obtain

$$\begin{aligned} u_{xyyy} + u_{xxxy} = {} & \frac{vy + 2r}{2vy^2} u_{xx} + \frac{\kappa(\theta + vy)}{v^2 y^2} u_{xy} - \frac{4\kappa(\theta - vy) + v^2}{2v^2 y} u_{xyy} \\ & - \frac{\rho v + 2r - vy}{vy} u_{xxy} - 2\rho u_{xxyy} - \frac{1}{2y} u_{xxx} + \frac{1}{vy^2} f_x - \frac{2}{vy} f_{xy}. \end{aligned} \tag{17}$$

Notice that all the terms in the right hand sides of (15)–(17) have compact $\mathcal{O}(h^2)$ approximations at node (i, j) using finite differences based on δ_x, δ_x^2, δ_y, δ_y^2. We have, for example, $u_{xxy_{i,j}} = \delta_x^2 \delta_y u_{i,j} + \mathcal{O}(h^2)$. By differentiating Eq. (12) twice with respect to x and y, respectively, and adding the two expressions, we obtain

$$\begin{aligned} u_{xxxx} + u_{yyyy} = {} & -2\rho u_{xyyy} - 2\rho u_{xxxy} - 2u_{xxyy} + 2\frac{(\kappa vy - v^2 - \kappa\theta)}{v^2 y} u_{xxy} - \frac{(2r - vy)}{vy} u_{xxx} \\ & + 2\frac{(\kappa vy - v^2 - \kappa\theta)}{v^2 y} u_{yyy} - \frac{(-vy + 4\rho v + 2r)}{vy} u_{xyy} + 4\frac{\kappa}{vy} u_{yy} + \frac{2}{y} u_{xy} - \frac{2}{vy}(f_{xx} + f_{yy}). \end{aligned} \tag{18}$$

Again, using (15)–(17), the right hand side can be approximated up to $\mathcal{O}(h^2)$ within the nine-point compact stencil. Substituting Eqs. (15)–(18) into Eq. (14) and simplifying yields a new expression for the error term $\tau_{i,j}$ that consists only of terms which are either

- terms of order $\mathcal{O}(h^4)$, or
- terms of order $\mathcal{O}(h^2)$ multiplied by derivatives of u which can be approximated up to $\mathcal{O}(h^2)$ within the nine-point compact stencil.

Hence, substituting the central $\mathcal{O}(h^2)$ approximations to the derivatives in this new expression for the error term and inserting it into (13) yields the following $\mathcal{O}(h^4)$ approximation to the initial partial differential equation (12)

$$\begin{aligned} & -\frac{1}{24} \frac{h^2((vy_j - 2r)^2 - 4\rho vr - 2\kappa(vy_j - \theta) - 2v^2) + 12v^2 y_j^2}{vy_j} \delta_x^2 u_{i,j} \\ & \quad - \frac{1}{12} \frac{h^2(2\kappa^2(vy_j - \theta)^2 - \kappa v^3 y_j - \kappa\theta v^2 - v^4) + 6v^4 y_j^2}{v^3 y_j} \delta_y^2 u_{i,j} - \frac{1}{12} h^2 v y_j (1 + 2\rho^2) \delta_x^2 \delta_y^2 u_{i,j} \\ & \quad + \frac{h^2}{6} \frac{(\kappa(vy_j - \theta) + v\rho(vy_j - 2r))}{v} \delta_x^2 \delta_y u_{i,j} + \frac{h^2}{12} \frac{(4\kappa\rho(vy_j - \theta) + v(vy_j - 2r))}{v} \delta_x \delta_y^2 u_{i,j} \\ & \quad - \frac{1}{6} \frac{h^2(\kappa(vy_j - 2r)(vy_j - \theta) - \kappa v^2 y_j \rho - v^3 \rho - v^2 r) + 6v^3 y_j^2 \rho}{v^2 y_j} \delta_x \delta_y u_{i,j} \\ & \quad + \frac{1}{12} \frac{6v^2 y_j^2 - 12vy_j r - h^2[v^2 + \kappa(vy_j - \theta)]}{vy_j} \delta_x u_{i,j} + \frac{\kappa}{6} \frac{(6v^2 y_j^2 - 6vy_j\theta - h^2[v^2 + \kappa(vy_j - \theta)])}{v^2 y_j} \delta_y u_{i,j} \\ & = f_{i,j} + \frac{h^2}{6} \frac{\rho}{v} \delta_x \delta_y f_{i,j} - \frac{h^2}{6} \frac{(v^2 + \kappa(vy_j - \theta))}{v^2 y_j} \delta_y f_{i,j} - \frac{h^2}{12} \frac{(2\rho v - 2r + vy_j)}{vy_j} \delta_x f_{i,j} + \frac{h^2}{12} \delta_x^2 f_{i,j} + \frac{h^2}{12} \delta_y^2 f_{i,j}. \end{aligned} \tag{19}$$

The fourth order compact finite difference scheme (19) considered at the mesh point (i, j) involves the nearest eight neighbouring mesh points. Associated to the shape of the computational stencil, we introduce indexes for each node from zero to nine,

$$\begin{pmatrix} u_{i-1,j+1} = u_6 & u_{i,j+1} = u_2 & u_{i+1,j+1} = u_5 \\ u_{i-1,j} = u_3 & u_{i,j} = u_0 & u_{i+1,j} = u_1 \\ u_{i-1,j-1} = u_7 & u_{i,j-1} = u_4 & u_{i+1,j-1} = u_8 \end{pmatrix}. \tag{20}$$

With this indexing, the scheme (19) is defined by

$$\sum_{l=0}^{8} \alpha_l u_l = \sum_{l=0}^{8} \gamma_l f_l, \tag{21}$$

where the coefficients α_l and γ_l are given by

$$\begin{aligned}
\alpha_0 &= \left(\frac{4\kappa^2+v^2}{12v} - \frac{v(2\rho^2-5)}{3h^2}\right) y_j - \frac{\kappa v^2 + 2\kappa^2\theta + v^2 r}{3v^2} + \frac{-v^4 + \kappa^2\theta^2 - v^3 r\rho + v^2 r^2}{3v^3 y_j},\\
\alpha_{1,3} &= \left(-\frac{v}{24} + \frac{\pm\frac{1}{6}v \mp \frac{1}{3}\kappa\rho}{h} + \frac{v(\rho^2-1)}{3h^2}\right) y_j \mp \frac{\kappa h}{24} + \frac{\kappa}{12} + \frac{r}{6}\\
&\quad \mp \frac{vr - \kappa\theta\rho}{3vh} \mp \frac{(v^2-\kappa\theta)h}{24vy_j} - \frac{-2rv\rho + \kappa\theta + 2r^2 - v^2}{12vy_j},\\
\alpha_{2,4} &= \left(-\frac{\kappa^2}{6v} + \frac{\pm\frac{1}{3}\kappa \mp \frac{1}{6}\rho v}{h} + \frac{v(\rho^2-1)}{3h^2}\right) y_j \mp \frac{\kappa^2 h}{12v} + \frac{\kappa(v^2+4\kappa\theta)}{12v^2}\\
&\quad \mp \frac{rv\rho - \kappa\theta}{3vh} \mp \frac{\kappa(v^2-\kappa\theta)h}{12v^2 y_j} + \frac{(2\kappa\theta+v^2)(v^2-\kappa\theta)}{12v^3 y_j},\\
\alpha_{5,7} &= \left(-\frac{\kappa}{24} \pm \frac{(2\rho+1)(2\kappa+v)}{24h} - \frac{v(\rho+1)(2\rho+1)}{12h^2}\right) y_j + \frac{\kappa(\rho v + 2r + \theta)}{24v}\\
&\quad \mp \frac{(2\rho+1)(\kappa\theta+vr)}{12vh} + \frac{v^2 r + v^3\rho - 2r\kappa\theta}{24v^2 y_j},\\
\alpha_{6,8} &= \left(\frac{\kappa}{24} \pm \frac{(2\rho-1)(-2\kappa+v)}{24h} - \frac{v(2\rho-1)(\rho-1)}{12h^2}\right) y_j - \frac{\kappa(\rho v + 2r + \theta)}{24v}\\
&\quad \mp \frac{(2\rho-1)(vr-\kappa\theta)}{12vh} - \frac{v^2 r + v^3\rho - 2r\kappa\theta}{24v^2 y_j},
\end{aligned}$$

and

$$\begin{aligned}
&\gamma_0 = \frac{2}{3}, \qquad \gamma_5 = \gamma_7 = \frac{\rho}{24}, \qquad \gamma_6 = \gamma_8 = -\frac{\rho}{24},\\
&\gamma_{1,3} = \frac{1}{12} \mp \frac{h}{24} \pm \frac{1}{12}\frac{(r-\rho v)h}{vy_j}, \qquad \gamma_{2,4} = \frac{1}{12} \mp \frac{1}{12}\frac{\kappa h}{v} \mp \frac{1}{12}\frac{(v^2-\kappa\theta)h}{v^2 y_j}.
\end{aligned}$$

When multiple indexes are used with $\pm$ and $\mp$ signs, the first index corresponds to the upper sign.

Remark 1. The derivation of the scheme in this section can be modified to accommodate other stochastic volatility models as, e.g. the GARCH diffusion model (3) or the 3/2-model (4). Using these models the structure of the partial differential equations (5), (11) and (12) remains the same, only the coefficients of the derivatives have to be modified accordingly. Similarly, the coefficients of the derivatives in (15)–(18) have to be modified. Substituting these in the modified expression for the truncation error one obtains equivalent $\mathcal{O}(h^4)$ approximations as (19).

4.2. High-order scheme for the parabolic problem

The high-order compact approach presented in the previous section can be extended to the parabolic problem directly by considering the time derivative in place of $f(x, y)$. Any time integrator can be implemented to solve the problem as presented in [18]. We consider the most common class of methods involving two time steps. For example, differencing at $t_\mu = (1-\mu)t^n + \mu t^{n+1}$, where $0 \le \mu \le 1$ and the superscript n denotes the time level, yields a class of integrators that include the forward Euler ($\mu = 0$), Crank–Nicolson ($\mu = 1/2$) and backward Euler ($\mu = 1$) schemes. We use the notation $\delta_t^+ u^n = \frac{u^{n+1}-u^n}{k}$. Then the resulting fully discrete difference scheme for node (i, j) at the time level n becomes

$$\sum_{l=0}^{8} \mu\alpha_l u_l^{n+1} + (1-\mu)\alpha_l u_l^n = \sum_{l=0}^{8} \gamma_l \delta_t^+ u_l^n,$$

that can be written in the form (after multiplying by $24v^3h^2yk$)

$$\sum_{l=0}^{8} \beta_l u_l^{n+1} = \sum_{l=0}^{8} \zeta_l u_l^n. \tag{22}$$

The coefficients β_l, ζ_l are numbered according to the indexes (20) and are given by

$$\begin{aligned}
\beta_0 &= (((2y_j^2-8)v^4+((-8\kappa-8r)y_j-8\rho r)v^3+(8\kappa^2y_j^2+8r^2)v^2-16\kappa^2\theta v y_j\\
&\quad +8\kappa^2\theta^2)\mu k+16v^3y_j)h^2+(-16\rho^2+40)y_j^2v^4\mu k\\
\beta_{1,3} &= \pm((\kappa\theta v^2-v^4-\kappa y_j v^3)\mu k-(y_j+2\rho)v^3+2v^2r)h^3+(((-y_j^2+2)v^4+((4r+2\kappa)y_j+4\rho r)v^3\\
&\quad -(2\kappa\theta+4r^2)v^2)\mu k+2v^3y_j)h^2\pm(4v^4y_j^2+(-8y_j^2\kappa\rho-8y_jr)v^3+8y_j\kappa\theta\rho v^2)\mu kh+(8\rho^2-8)y_j^2v^4\mu k,\\
\beta_{2,4} &= \pm((2\kappa^2\theta v-2\kappa^2v^2y_j-2v^3\kappa)\mu k-2v^2y_j\kappa+2v\kappa\theta-2v^3)h^3+((2v^4+2\kappa y_jv^3\\
&\quad +(-4\kappa^2y_j^2+2\kappa\theta)v^2+8\kappa^2\theta v y_j-4\kappa^2\theta^2)\mu k+2v^3y_j)h^2\\
&\quad \pm((8y_j^2\kappa+8y_j\rho r)v^3-4v^4y_j^2\rho-8v^2y_j\kappa\theta)\mu kh+(8\rho^2-8)y_j^2v^4\mu k,\\
\beta_{5,7} &= ((v^4\rho+(-y^2\kappa+\kappa y_j\rho+r)v^3+(\theta+2r)\kappa y_jv^2-2r\kappa\theta v)\mu k+v^3\rho y_j)h^2\pm((2\rho+1)y_j^2v^4\\
&\quad +((2+4\rho)\kappa y_j^2+(-4\rho r-2r)y_j)v^3+(-2\theta-4\theta\rho)\kappa y_jv^2)\mu kh+(-2-4\rho^2-6\rho)y_j^2v^4\mu k,\\
\beta_{6,8} &= ((-v^4\rho+(y_j^2\kappa-\kappa y_j\rho-r)v^3+(-\theta-2r)\kappa y_jv^2+2r\kappa\theta v)\mu k-v^3\rho y_j)h^2\pm((2\rho-1)y_j^2v^4\\
&\quad +((2-4\rho)\kappa y_j^2+(2r-4\rho r)y_j)v^3+(4\theta\rho-2\theta)\kappa y_jv^2)\mu kh+(-4\rho^2+6\rho-2)y_j^2v^4\mu k,
\end{aligned}$$

and

$$\begin{aligned}
\zeta_0 &= 16v^3y_jh^2+(1-\mu)k(((8-2y_j^2)v^4+((8\kappa+8r)y_j+8\rho r)v^3\\
&\quad +(-8r^2-8\kappa^2y_j^2)v^2+16\kappa^2\theta v y_j-8\kappa^2\theta^2)h^2+(-40+16\rho^2)y_j^2v^4),\\
\zeta_{1,3} &= \pm(2r-(y_j+2\rho)v)v^2h^3+2v^3y_jh^2+(1-\mu)k(\pm(v\kappa y_j+v^2-\kappa\theta)v^2h^3+(v^2y_j^2-(4r+2\kappa)vy_j\\
&\quad +4r^2+2\kappa\theta-2v^2-4\rho vr)v^2h^2\pm((-4v+8\kappa\rho)v^3y_j^2+(-8\kappa\theta\rho+8vr)v^2y_j)h+(8v^2-8v^2\rho^2)v^2y_j^2),\\
\zeta_{2,4} &= \pm(2v\kappa\theta-2v^2y_j\kappa-2v^3)h^3+2v^3y_jh^2+(1-\mu)k(\pm2(v^3\kappa-\kappa^2\theta v\\
&\quad +\kappa^2v^2y_j)h^3+(4\kappa^2v^2y_j^2-(2v^2+8\kappa\theta)\kappa vy_j+2\kappa\theta(2\kappa\theta-v^2)-2v^4)h^2\\
&\quad \pm((-8v^3\kappa+4v^4\rho)y_j^2+(8\kappa\theta v^2-8v^3\rho r)y_j)h+(-8v^4\rho^2+8v^4)y_j^2),\\
\zeta_{5,7} &= v^3\rho y_jh^2+(1-\mu)k((v^3y_j^2\kappa-v(v\kappa\theta+2r\kappa v+\kappa v^2\rho)y_j-v(v^2r-2r\kappa\theta+v^3\rho))h^2\pm(-v(2v^3\rho+v^3\\
&\quad +4\kappa v^2\rho+2v^2\kappa)y_j^2+v(2v\kappa\theta+4v\kappa\theta\rho+4v^2\rho r+2v^2r)y_j)h+v(2v^3+6v^3\rho+4v^3\rho^2)y_j^2),\\
\zeta_{6,8} &= -v^3\rho y_jh^2+(1-\mu)k((-v^3y_j^2\kappa+v(v\kappa\theta+2r\kappa v\\
&\quad +\kappa v^2\rho)y_j+v(v^2r-2r\kappa\theta+v^3\rho))h^2\pm(v(-2v^3\rho+v^3\\
&\quad +4\kappa v^2\rho-2v^2\kappa)y_j^2+v(2v\kappa\theta-4v\kappa\theta\rho+4v^2\rho r-2v^2r)y_j)h+v(2v^3-6v^3\rho+4v^3\rho^2)y_j^2).
\end{aligned}$$

When multiple indexes are used with $\pm$ and $\mp$ signs, the first index corresponds to the upper sign. Choosing $\mu = 1/2$, i.e. in the Crank–Nicolson case, the resulting scheme is of order two in time and of order four in space.

4.3. Stability analysis

Besides the multi-dimensionality the initial-boundary-value problem (22) features two main difficulties for its stability analysis: the coefficients are non-constant and the boundary conditions are not periodic. In this section, we consider the von Neumann stability analysis (see, e.g. [19]) even if the problem considered does not satisfy periodic boundary conditions. This approach is extensively used in the literature and yields good criteria on the robustness of the scheme. Other approaches which take into account the boundary conditions like normal mode analysis [20] are beyond the scope of the present paper (we refer to [21] for normal mode analysis for a high-order compact scheme).

To consider the variable coefficients, the principle of 'frozen coefficients' (the variable coefficient problem is stable if all the 'frozen' problems are stable) [20,19] is employed. It should be noted, that in the discrete case, this principle is far from trivial. The most general statements are given in [20,22–24] and references therein for hyperbolic problems. For parabolic problems in the discrete case we refer to [25,26]. Using the frozen coefficients approach gives a necessary stability condition and slightly strengthened stability for frozen coefficients is sufficient to ensure overall stability [25].

We now turn to the von Neumann stability analysis. We rewrite $u_{i,j}^n$ as

$$u_{i,j}^n = g^n e^{Iiz_1+Ijz_2}, \tag{23}$$

where I is the imaginary unit, g^n is the amplitude at time level n, and $z_1 = 2\pi h/\lambda_1$ and $z_2 = 2\pi h/\lambda_2$ are phase angles with wavelengths λ_1 and λ_2, in the range $[0, 2\pi[$, respectively. Then the scheme is stable if for all z_1 and z_2 the amplification factor $G = g^{n+1}/g^n$ satisfies the relation

$$|G|^2 - 1 \le 0. \tag{24}$$

An expression for G can be found using (23) in (22).

Our aim is to prove von Neumann stability (for 'frozen coefficients') without restrictions on the time step size. To show that (24) holds we would need to study the (formidable) expression for the amplification factor G (not given here) which

consists of polynomials of order up to six in 13 variables. To reduce the high number of parameters in the following numerical analysis, we assume here zero interest rate $r = 0$ and choose the parameter $\mu = 1/2$ (Crank–Nicolson case). Even then, at present a complete analysis for non-zero correlation seems out of reach, but we are able to show the following result.

Theorem 1. *For $r = \rho = 0$ and $\mu = 1/2$ (Crank–Nicolson), the scheme (22) satisfies the stability condition (24).*

Proof. Let us define new variables

$$c_1 = \cos\left(\frac{z_1}{2}\right), \qquad c_2 = \cos\left(\frac{z_2}{2}\right), \qquad s_1 = \sin\left(\frac{z_1}{2}\right), \qquad s_2 = \sin\left(\frac{z_2}{2}\right),$$
$$W = \frac{2\,(\theta - vy)}{v} s_2, \qquad V = \frac{2vy}{\kappa} s_1,$$

which allow us to express G in terms of h, k, κ, V, W and trigonometric functions only. This reduces the number of variables in the amplification factor from ten to nine. The new variable V has a constant positive sign contrary to W.

In the new variables the stability criterion (24) of the scheme can be written as

$$\frac{-8kh^2(n_4h^2 + n_2)}{d_6h^6 + d_4h^4 + d_2h^2 + d_0} \le 0, \tag{25}$$

with

$$n_4 = -4\,V\kappa^3 f_3\, s_1^3 W^2 - V^3\kappa^3 f_4\, s_1^3, \qquad n_2 = -4\,V^3\kappa^3 f_2\, f_1\, s_1,$$
$$d_6 = 4\,\left(-2\,Wc_2 + Vc_1\right)^2 \kappa^2 s_1^4,$$
$$d_4 = \frac{1}{4}\,\kappa^4 s_1^4 \left(V^2 - 4\,Vc_1\,Wc_2 + 4\,W^2\right)^2 k^2 - 4\,V\kappa^3 s_1^3 \left(f_4\,V^2 + 4\,f_3\,W^2\right) k + 16\,\kappa^2 V^2 f_2^2 s_1^2,$$
$$d_2 = V^2\kappa^4 s_1^2 \left(V^2 f_6 - 36\,Vc_1\,Wc_2 + 4\,f_5\,W^2\right) k^2 - 16\,V^3\kappa^3 f_2\, f_1\, s_1\, k,$$
$$d_0 = 4V^4\kappa^4 f_1^2 k^2,$$

where f_1, f_2, f_3, f_4, f_5, and f_6 have constant sign and are defined by

$$f_1 = 2c_1^2c_2^2 + c_1^2 + c_2^2 - 4 \le 0, \qquad f_2 = c_1^2 + c_2^2 + 1 \ge 0,$$
$$f_3 = 2c_1^2c_2^2 - c_1^2 - 1 \le 0, \qquad f_4 = 2c_1^2c_2^2 - c_2^2 - 1 \le 0,$$
$$f_5 = 4c_1^4c_2^2 - 2c_1^2 - c_2^2 + 8 \ge 0, \qquad f_6 = 4c_1^2{c_2}^4 - 2c_2^2 - c_1^2 + 8 \ge 0.$$

We observe that we can restrict our analysis (except for d_2, treated below) to the trigonometric functions s_1, s_2, c_1, and c_2 in the reduced range $[0, 1]$ ($z_1/2$ and $z_2/2$ are in $[0, \pi[$, even exponents for cosinus functions). It is straight-forward to verify that n_4, n_2, d_6, d_4, and d_0 are positive. It remains to prove $d_2 = d_{22}k^2 + d_{21}k$ is positive as well. Indeed, $d_{21} \ge 0$ and d_{22} is a polynomial of degree two in W having a positive leading order coefficient. The minimum value of d_{22} is given by

$$m = 2V^4\kappa^4 s_1^2 f_1 f_7 / f_5$$

with $f_7 = 4c_2^4c_1^4 - 2c_1^4c_2^2 - 2c_1^2c_2^4 + 6c_1^2c_2^2 + c_1^2 + c_2^2 - 8 \le 0$. Hence, m is positive and then d_2 is positive as well. Therefore, the numerator in (25) is negative and the denominator in (25) is positive which completes the proof. □

For non-zero correlation the situation becomes more involved. Additional terms appear in the expression for the amplification factor G and we face an additional degree of freedom through ρ. Since we have proven condition (24) for $\rho = 0$ it seems reasonable to assume it also holds at least for values of ρ close to zero. In practical applications, however, correlation can be strongly negative. Few theoretical results can be obtained, we recall the following lemma from [27].

Lemma 2. *For any ρ, $r = 0$, and $\mu = 1/2$ (Crank–Nicolson) it holds: if either $c_1 = \pm 1$ or $c_2 = \pm 1$ or $y = 0$, then the stability condition (24) is satisfied.*

Proof. See Lemma 1 in [27]. □

In [27], we have reformulated condition (24) into a constrained optimisation problem and have employed a line-search global-optimisation algorithm to find the maxima. We have found that the stability condition (24) was always satisfied. The maxima for each $\rho \in [-1, 0]$ were always negative but very close to zero. This result is in agreement with Lemma 2 (in fact, $|G|^2 - 1 = 0$ for $y = 0$). Our conjecture from these results is that the stability condition (24) is satisfied also for non-vanishing correlation although it will be hard to give an analytical proof.

In our numerical experiments we observe stability also for a general choice of parameters. To validate the stability property of the scheme also for general parameters, we perform additional numerical tests in Section 5.

Table 1
Default parameters for numerical simulations.

Parameter	Value
Strike price	$K = 100$
Time to maturity	$T = 0.5$
Interest rate	$r = 0.05$
Volatility of volatility	$v = 0.1$
Mean reversion speed	$\kappa = 2$
Long-run mean of σ	$\theta = 0.1$
Correlation	$\rho = -0.5$

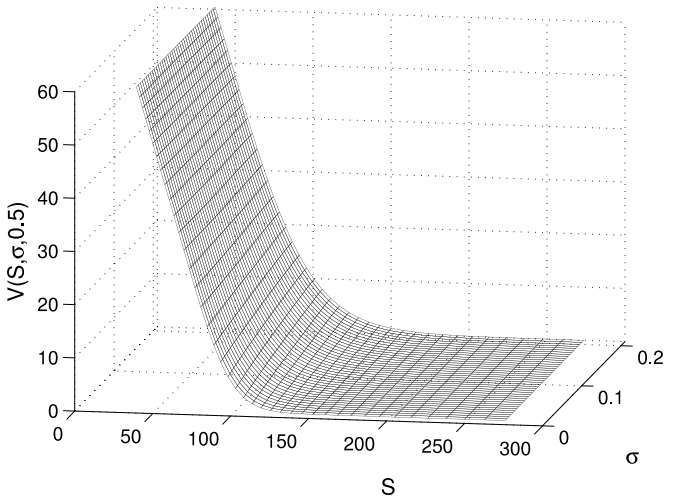

Fig. 1. Numerical solution for the European option price.

5. Numerical results

5.1. Numerical convergence

In this section we perform a numerical study to compute the order of convergence of the scheme (22). Due to the compact discretisation the resulting linear systems have a good sparsity pattern and can be solved very efficiently. We compute the l_2 norm error ε_2 and the maximum norm error ε_∞ of the numerical solution with respect to a numerical reference solution on a fine grid. We fix the parabolic mesh ratio k/h^2 to a constant value which is natural for parabolic PDEs and our scheme which is of order $\mathcal{O}(k^2)$ in time and $\mathcal{O}(h^4)$ in space. Then, asymptotically, we expect these errors to converge as $\varepsilon = Ch^m$ for some m and C representing constants. This implies $\ln(\varepsilon) = \ln(C) + m\ln(h)$. Hence, the double-logarithmic plot ε against h should be asymptotic to a straight line with slope m. This gives a method for experimentally determining the order of the scheme.

Fig. 1 shows the numerical solution for the European option price at time $T = 0.5$ using the parameters from Table 1.

We refer to Figs. 2 and 3 for the results of the numerical convergence study using the default parameters from Table 1. For the parameter μ, we use a Rannacher time-stepping choice [28], i.e. we start with four fully implicit quarter time steps ($\mu = 1$) and then continue with Crank–Nicolson ($\mu = 1/2$). For comparison we conducted additional experiments using a standard, second order scheme (based on the central difference discretisation (13) where we neglect the truncation error). We observe that the numerical convergence order agrees well with the theoretical order of the schemes. It is important to choose the mesh in such a way that the singular point of the initial condition is not a point of the mesh. The construction of such a mesh is always possible in a simple manner. Then the non-smooth payoff can be directly considered in our scheme and we observe fourth order numerical convergence.

Remark 2. Without constraint on the mesh, i.e. when the singular point of the payoff is a mesh point, the rate of convergence is reduced to two. However, it is possible to recover the fourth order convergence with such a mesh if the initial data are smoothed.

The numerical convergence analysis also shows the superior efficiency of the high-order scheme compared to a standard second order discretisation. In each time step of each scheme a linear system has to be solved. For both schemes this requires the same computational time for the same dimension. To achieve the same level of accuracy the new scheme requires significantly less grid points, or in other words, the computational time to obtain a given accuracy level is greatly reduced by using the high-order scheme.

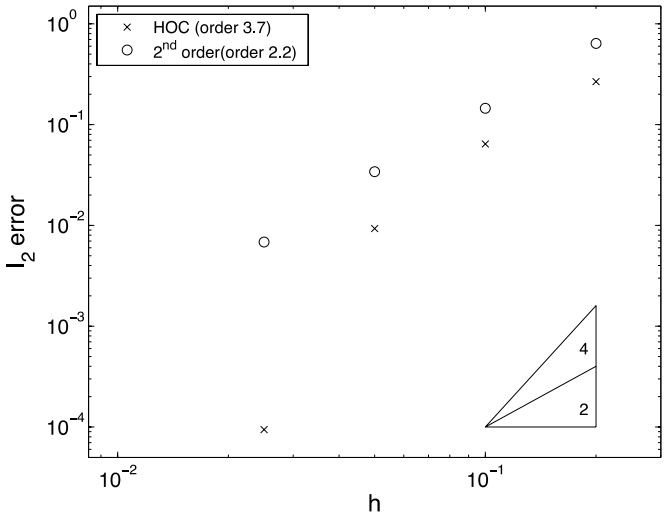

Fig. 2. l_2-error vs. h.

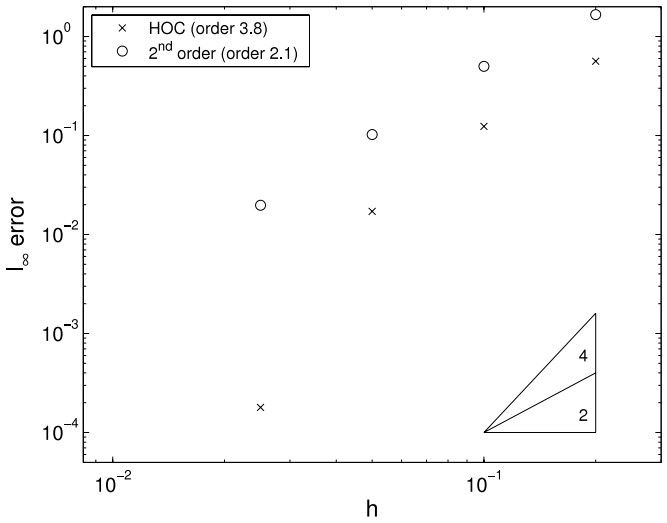

Fig. 3. l_∞-error vs. h.

5.2. Numerical stability analysis

In our numerical analysis in Section 4.3, we have proven the stability result Theorem 1 for $r = \rho = 0$. To validate this property for general parameters, we perform additional numerical tests. We compute numerical solutions for varying values of the parabolic mesh ratio k/h^2 and the mesh width h. Plotting the associated l_2 norm errors in the plane should allow us to detect stability restrictions depending on k/h^2 or oscillations that occur for high cell Reynolds number (large h). This approach for a numerical stability study was also used in [8]. We perform numerical experiments for $\rho = 0$ and $\rho = -0.5$. For the other parameters, we use again the default parameters from Table 1. The results are shown in Fig. 4. For both cases, $\rho = 0$ and $\rho = -0.5$, the errors show a similar behaviour, being slightly larger for non-vanishing correlation. There is almost no dependence of the error on the parabolic mesh ratio k/h^2, which confirms numerically regular solutions can be obtained without restriction on the time step size. For larger values of h, which also result in a higher cell Reynolds number, the error grows gradually, and no oscillation in the numerical solutions occurs. Based on these results and the findings in [27], we conjecture that the stability condition (24) also holds for general choice of parameters.

6. Conclusion

We have presented a new high-order compact finite difference scheme for option pricing under stochastic volatility that is fourth order accurate in space and second order accurate in time. We have conducted a von Neumann stability analysis (for 'frozen coefficients' and periodic boundary data) and proved unconditional stability for vanishing correlation. In our

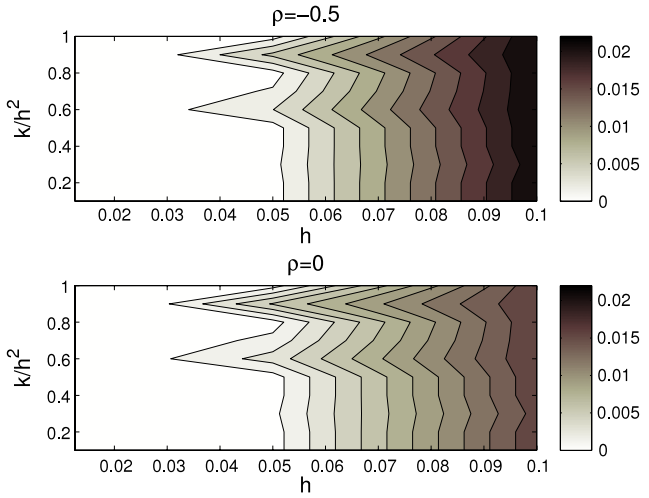

Fig. 4. l_2 norm error in the k/h^2-h-plane for $\rho = -0.5$ (top) and $\rho = 0$ (bottom).

numerical experiments we observe a stable behaviour also for a general choice of parameters. Additional numerical tests presented here and the results of subsequent research reported in [27] suggest that the scheme is also von Neumann stable for non-zero correlation. In our numerical convergence study we obtain fourth order numerical convergence for the non-smooth payoffs which are typical in option pricing.

It would be interesting to consider extensions of this scheme to non-uniform grids and to the American option pricing problem, where early exercise of the option is possible. An approach to the first would be to introduce a transformation of the partial differential equation from a non-uniform grid to a uniform grid [29]. Then our high order compact methodology can be applied to this transformed partial differential equation. This is, however, not straightforward as the derivatives of the transformation appear in the truncation error and due to the presence of the cross-derivative terms. One cannot proceed to cancel terms in the truncation error in a similar fashion as in the current paper, and the derivation of a high-order compact scheme becomes much more involved. For the second extension, the American option pricing problem, one has to solve a free boundary problem. It can be written as a linear complementarity problem which can be discretised using the scheme (22). To retain the high-order convergence one would need to combine the high-order discretisation with a high-order resolution of the free boundary. Both extensions are beyond the scope of the present paper, and we leave them for future research.

Acknowledgments

Bertram Düring acknowledges partial support from the Austrian Science Fund (FWF), grant P20214, and from the Austrian–Croatian Project HR 01/2010 of the Austrian Exchange Service (ÖAD). The authors are grateful to the anonymous referees for helpful remarks and suggestions.

References

[1] F. Black, M. Scholes, The pricing of options and corporate liabilities, J. Polit. Econ. 81 (1973) 637–659.
[2] S.L. Heston, A closed-form solution for options with stochastic volatility with applications to bond and currency options, Rev. Finan. Stud. 6 (2) (1993) 327–343.
[3] B. Düring, Asset pricing under information with stochastic volatility, Rev. Deriv. Res. 12 (2) (2009) 141–167.
[4] E. Benhamou, E. Gobet, M. Miri, Time dependent Heston model, SIAM J. Financ. Math. 1 (2010) 289–325.
[5] D. Tavella, C. Randall, Pricing Financial Instruments: The Finite Difference Method, John Wiley & Sons, 2000.
[6] D.Y. Tangman, A. Gopaul, M. Bhuruth, Numerical pricing of options using high-order compact finite difference schemes, J. Comput. Appl. Math. 218 (2) (2008) 270–280.
[7] B. Düring, M. Fournié, A. Jüngel, Convergence of a high-order compact finite difference scheme for a nonlinear Black–Scholes equation, Math. Modelling Numer. Anal. 38 (2) (2004) 359–369.
[8] B. Düring, M. Fournié, A. Jüngel, High-order compact finite difference schemes for a nonlinear Black–Scholes equation, Int. J. Theor. Appl. Finance 6 (7) (2003) 767–789.
[9] W. Liao, A.Q.M. Khaliq, High-order compact scheme for solving nonlinear Black–Scholes equation with transaction cost, Int. J. Comput. Math. 86 (6) (2009) 1009–1023.
[10] R. Zvan, P.A. Forsyth, K.R. Vetzal, Penalty methods for American options with stochastic volatility, J. Comput. Appl. Math. 91 (2) (1998) 199–218.
[11] N. Clarke, K. Parrott, Multigrid for American option pricing with stochastic volatility, Appl. Math. Finance 6 (3) (1999) 177–195.
[12] N. Hilber, A. Matache, C. Schwab, Sparse wavelet methods for option pricing under stochastic volatility, J. Comput. Finance 8 (4) (2005) 1–42.
[13] W. Zhu, D.A. Kopriva, A spectral element approximation to price European options with one asset and stochastic volatility, J. Sci. Comput. 42 (3) (2010) 426–446.
[14] S. Ikonen, J. Toivanen, Efficient numerical methods for pricing American options under stochastic volatility, Numer. Methods Partial Differential Equations 24 (1) (2008) 104–126.

[15] K.J. in't Hout, S. Foulon, ADI finite difference schemes for option pricing in the Heston model with correlation, Int. J. Numer. Anal. Model. 7 (2010) 303–320.
[16] P. Kangro, R. Nicolaides, Far field boundary conditions for Black–Scholes equations, SIAM J. Numer. Anal. 38 (2000) 1357–1368.
[17] B. Gustafsson, The convergence rate for difference approximation to general mixed initial-boundary value problems, SIAM J. Numer. Anal. 18 (2) (1981) 179–190.
[18] W.F. Spotz, C.F. Carey, Extension of high-order compact schemes to time-dependent problems, Numer. Methods Partial Differential Equations 17 (6) (2001) 657–672.
[19] J.C. Strikwerda, Finite Difference Schemes and Partial Differential Equations, second ed., Society for Industrial and Applied Mathematics (SIAM), Philadelphia, PA, 2004.
[20] B. Gustafsson, H.-O. Kreiss, J. Oliger, Time Dependent Problems and Difference Methods, Wiley-Interscience, 1996.
[21] M. Fournié, A. Rigal, High order compact schemes in projection methods for incompressible viscous flows, Commun. Comput. Phys. 9 (4) (2011) 994–1019.
[22] S. Mishra, M. Svärd, On stability of numerical schemes via frozen coefficients and the magnetic induction equations, BIT Numer. Math. 50 (2010) 85–108.
[23] B.A. Wade, Symmetrizable finite difference operators, Math. Comp. 54 (1990) 525–543.
[24] J.C. Strikwerda, B.A. Wade, An extension of the Kreiss matrix theorem, SIAM J. Numer. Anal. 25 (6) (1988) 1272–1278.
[25] R.D. Richtmyer, K.W. Morton, Difference Methods for Initial Value Problems, Interscience, New York, 1967.
[26] O.B. Widlund, Stability of parabolic difference schemes in the maximum norm, Numer. Math. 8 (1966) 186–202.
[27] B. Düring, M. Fournié, On the stability of a compact finite difference scheme for option pricing, in: M. Günther, et al. (Eds.), Progress in Industrial Mathematics at ECMI 2010, Springer, Berlin, Heidelberg, 2012, pp. 215–221.
[28] R. Rannacher, Finite element solution of diffusion problems with irregular data, Numer. Math. 43 (2) (1984) 309–327.
[29] M. Fournié, High order conservative difference methods for 2d drift-diffusion model on non-uniform grid, Appl. Numer. Math. 33 (1–4) (2000) 381–392.